

## Controlled directional ion emission from several fragmentation channels of CO driven by a few-cycle laser field

K. J. Betsch,<sup>1,2,\*</sup> Nora G. Johnson,<sup>1,3</sup> B. Bergues,<sup>1</sup> M. Kübel,<sup>1</sup> O. Herrwerth,<sup>1</sup> A. Senftleben,<sup>4</sup> I. Ben-Itzhak,<sup>3</sup> G. G. Paulus,<sup>5,6</sup> R. Moshhammer,<sup>4</sup> J. Ullrich,<sup>4,7</sup> M. F. Kling,<sup>1,3</sup> and R. R. Jones<sup>2</sup>

<sup>1</sup>Max-Planck-Institut für Quantenoptik, D-85748 Garching, Germany

<sup>2</sup>Department of Physics, University of Virginia, Charlottesville, Virginia 22904-4714, USA

<sup>3</sup>J. R. Macdonald Laboratory, Department of Physics, Kansas State University, Manhattan, Kansas 66506, USA

<sup>4</sup>Max-Planck-Institut für Kernphysik, D-69117 Heidelberg, Germany

<sup>5</sup>Friedrich-Schiller-Universität Jena, Max-Wien Platz 1, D-07743 Jena, Germany

<sup>6</sup>Helmholtz Institut Jena, D-07743 Jena, Germany

<sup>7</sup>Physikalisch-Technische Bundesanstalt, D-38116 Braunschweig, Germany

(Received 25 April 2012; published 5 December 2012)

We explore the dissociative ionization of CO with carrier-envelope-phase (CEP) tagged few-cycle laser pulses. We observe the CEP dependence of the directional emission of  $C^{p+}$  and  $O^{q+}$  fragments from transient  $CO^{(p+q)+}$  ions, where  $p + q \leq 3$  and  $q \leq 1$ . At  $I_0 = 3.5 \times 10^{14}$  W/cm<sup>2</sup>, a 180° phase difference between the  $C^+$  and  $O^+$  fragments from the ( $p = 1, q = 0$ ) and ( $p = 0, q = 1$ ) channels reflects the orientation dependence of the CO ionization. At  $I_0 = 1.2 \times 10^{15}$  W/cm<sup>2</sup>, we find a ~35° phase shift between the  $C^{2+}$  fragments from the ( $p = 2, q = 0$ ) and ( $p = 2, q = 1$ ) channels, in contrast to the 180° shift previously observed between the  $C^{2+}$  fragment channels at  $I_0 = 6 \times 10^{14}$  W/cm<sup>2</sup> [Phys. Rev. Lett. **106**, 073004 (2011)].

DOI: 10.1103/PhysRevA.86.063403

PACS number(s): 33.80.Wz

### I. INTRODUCTION

Optical control of molecular processes has been a topic of intense research for the past two decades. Historically, the laser pulse duration, frequency, phase, and polarization have been the common control knobs [1], but if the pulse duration is sufficiently short to approach the few-cycle regime, the laser waveform itself becomes important. Consider the electric field of a laser pulse  $E(t) = E_0(t) \cos(\omega t + \phi)$ , where  $E_0(t)$  is the time-dependent envelope,  $\omega$  is the central frequency, and  $\phi$  is the carrier-envelope phase (CEP). The CEP can be used to control the electric field waveform and has been successfully applied to, for example, control charge localization in the dissociative ionization of molecules [2–7]. The CEP adds a new dimension to existing control parameters and offers the potential to control chemical reactions by steering electronic motion inside the molecules, enabling charge-directed reactivity [8]. To date, most experimental CEP-controlled molecular dissociation studies, both on the relatively simple hydrogen molecule isotopologues [2–6] and the multielectron CO molecule [7], have focused on dissociative ionization channels where one of the fragments is neutral (e.g.,  $CO^+ \rightarrow C^+ + O$ ). However, as the laser intensity is increased, multiple ionization can occur, producing, in the case of diatomic molecules, two (highly) charged fragments. The exact pathways leading to a specific dissociation channel are often difficult to identify, although models such as Floquet theory have had some success [9–11].

Only very recently, a first study has been reported on the CEP control of the fragmentation of CO from several charge states [12]. Using 4.2 fs, 740 nm CEP-stabilized pulses at an intensity of  $6 \times 10^{14}$  W/cm<sup>2</sup> and a reaction microscope (REMI), Liu *et al.* observed that the emission directions

of  $C^{2+}$  ions from the dissociative ionization and Coulomb explosion channels were 180° out of phase. This opposite phase dependence was qualitatively described as being the result of competition between recollision excitation (leading to the dissociative ionization channel,  $CO^{2+} \rightarrow C^{2+} + O$ ) and recollision ionization (leading to the Coulomb-explosion channel  $CO^{3+} \rightarrow C^{2+} + O^+$ ) when a tunnel-ionized electron returns to the ion core. In the present study, we have further investigated the CEP control of the fragmentation of CO at different laser intensities, which may involve different mechanisms for fragmentation into the same channels. High sensitivity in the detection of CEP effects for various breakup channels is achieved by tagging the CEP for each and every laser shot in combination with single-shot detection of ions from the fragmentation of CO. In particular, we observe the CEP dependence of the breakup channels originating from  $CO^{Q+}$  with  $1 \leq Q \leq 3$ , enabling us to measure relative phase shifts in the CEP control between multiple channels. Throughout this work, the notation ( $p, q$ ) is used to represent the  $CO^{(Q=p+q)+} \rightarrow C^{p+} + O^{q+}$  channel.

### II. EXPERIMENTAL SETUP

The experimental setup, which consists of a few-cycle laser source, a reaction microscope [13], and a single-shot phase meter [14], has been previously described in detail [15,16]. Briefly, linearly polarized sub-5-fs laser pulses with central wavelength  $\lambda_0 = 750$  nm and an energy of 400  $\mu$ J are generated at a repetition rate of 3 kHz. Approximately 30  $\mu$ J of the pulse energy is focused into the phase meter, and the rest is attenuated with an iris and focused into a cold CO gas jet target inside the REMI spectrometer. The laser polarization is parallel to the spectrometer axis. The pulse durations for the phase meter and the REMI are minimized by pairs of fused silica wedges. In the phase meter, electrons are generated in the

\*kjbettsch@phys.ksu.edu

ionization of xenon atoms and directed towards two opposed (left and right) time-of-flight detectors aligned along the laser polarization direction. From comparison of the electron spectra on the left and right detectors, the relative CEP of each individual laser pulse is determined [14].

Inside the REMI, ions created by the laser pulse are extracted towards a position- and time-sensitive delay line microchannel plate detector. From the time and position information, the ion's momentum at the moment of dissociation is reconstructed. If the break-up channel creates two charged species, momentum conservation can be used to isolate two ions resulting from the fragmentation of a single molecule (coincidence filtering). Because the CEP and molecular dissociation data is recorded simultaneously, the results of each molecular dissociation event can be tagged with the laser pulse's CEP [15], allowing observation of effects of the pulse waveform on the fragmentation process. The primary advantage of using this phase-tagging method, the quality of which is discussed in detail in Refs. [15,17,18], as opposed to the more common CEP-locking method is the significant increase in data acquisition time that is afforded by the free-running laser. For example, the data presented in this work was collected over a period of up to 12 hours in order to ensure adequate statistics. It would be difficult to achieve comparable long-term stability from current CEP-locking technology.

The laser peak intensity,  $I_0 = E_0^2/(4\pi\alpha) = 2I$ , where  $\alpha$  is the fine structure constant and  $I$  is the cycle-averaged laser intensity, is estimated from auxiliary measurements performed immediately after the CO experiments, namely, the  $2U_p$  cutoff in the recoil energy spectrum of  $\text{Ar}^{2+}$  ions from the above-threshold ionization of argon [19,20]. Here,  $U_p$  is the ponderomotive energy obtained by an electron in the laser field and  $U_p = E_0^2/(4\omega^2)$  (atomic units are used throughout the paper unless otherwise specified). Comparison of the experimentally observed CEP dependence of the  $\text{Ar}^+$  and  $\text{Ar}^{2+}$  ion momenta with semiclassical calculations (see Ref. [21] for details) verifies the peak intensity and allows us to estimate the pulse duration as  $4.7(\pm 0.3)$  fs.

### III. RESULTS

Figure 1 shows the kinetic energy release (KER =  $E_C + E_O$ , where  $E_C$  and  $E_O$  are the energies of the carbon and oxygen fragments) spectra for the observed fragmentation channels of CO at two laser intensities. The  $\text{C}^{2+}$  ion was visible only at the higher intensity,  $I_0 = 1.2(\pm 0.1) \times 10^{15}$  W/cm<sup>2</sup>, while the  $\text{C}^+$  and  $\text{O}^+$  ions were observed at both intensities. In Fig. 1, we show the  $\text{C}^+$  and  $\text{O}^+$  KER spectra recorded at  $I_0 = 3.5(\pm 0.6) \times 10^{14}$  W/cm<sup>2</sup> because this data is cleaner than that obtained at the higher intensity. The solid lines represent the data which has not been coincidence filtered, for which the KER is determined by assuming momentum conservation between the detected and the nondetected fragment. Filtering the data for the coincident detection of both ions (dashed lines) allows us to unambiguously identify the channels which involve two charged species. Approximately 0.1% of the  $\text{O}^+$  fragments from the (1, 1) channel pass our (2, 1) coincidence filter due to the similar energy of the (1, 1) and (2, 0) channels, as can be seen by the small contribution below 10 eV in the blue dashed curve in Fig. 1(a). Three (1, 1) KER peaks are easily

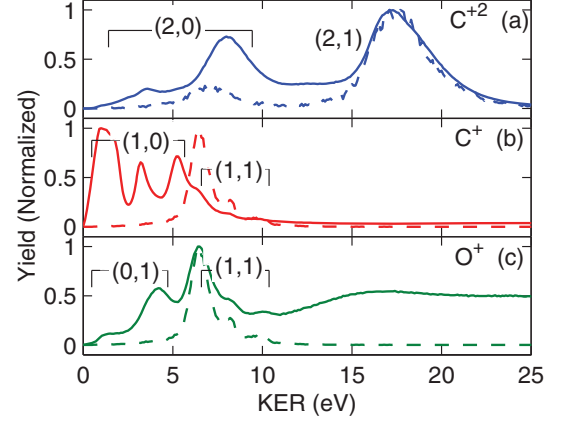


FIG. 1. (Color online) Measured kinetic energy release spectra for various fragmentation channels of CO. Noncoincident data are shown as solid lines, and data employing coincidence filtering for the (1, 1) and (2, 1) channels are shown as dashed lines. All curves have been normalized to the largest peak. Channel assignments are annotated above the curves. The  $\text{C}^{2+}$  data were obtained at  $I_0 = 1.2 \times 10^{15}$  W/cm<sup>2</sup>, and the  $\text{C}^+$  and  $\text{O}^+$  data at  $I_0 = 3.5 \times 10^{14}$  W/cm<sup>2</sup>. The high-energy tail in the noncoincident  $\text{O}^+$  yield (solid green line) is due to contamination from the  $\text{C}^+$  ions caused by overlap of the two species in time of flight. Table I lists the KER for all observed channels.

observable in the coincidence data. Previously, these were attributed to dissociation channels originating from different excited states of the  $\text{CO}^{2+}$  cation [22–25]; however, ongoing analysis suggests that they may also be due to above-threshold dissociation [26,27]. The observation of multiple (1, 0) peaks is consistent with previous work employing few-cycle pulses [7], where the spectral features could be reproduced by theoretical calculations incorporating laser-induced coupling between the (1, 0) and (0, 1) channels [7,28]. Two (0, 1) channels, which are energetically less favorable than the (1, 0) channels, are also observed for both laser intensities. The  $\text{C}^+$  fragments are more abundant than the  $\text{O}^+$  fragments by a factor of 7 (4) for the low (high) laser intensity.

The dependence of the directional emission of  $\text{C}^{2+}$  fragments upon the CEP is illustrated in Fig. 2. Figure 2(a) shows the momentum spectra [ $p_{\text{tot}} = (p_x^2 + p_y^2 + p_z^2)^{1/2}$ ] for all detected  $\text{C}^{2+}$  ions and the coincidence-filtered ions for the (2, 1) channel. For these momenta, Fig. 2(b) displays a density plot of the CEP-dependent asymmetry in the noncoincidence ion emission,

$$A(p_{\text{tot}}, \phi) = \frac{Y_f(p_{\text{tot}}, \phi) - Y_b(p_{\text{tot}}, \phi)}{Y_f(p_{\text{tot}}, \phi) + Y_b(p_{\text{tot}}, \phi)}, \quad (1)$$

where  $Y_f(p_{\text{tot}}, \phi)$  [ $Y_b(p_{\text{tot}}, \phi)$ ] is the ion yield within a specific phase and momentum bin for negative [positive]  $p_z$ . Comparison with the total momentum spectra in Fig. 2(a) indicates strong CEP-dependent modulations in the directional emission of  $\text{C}^{2+}$  fragments from the (2, 0) and (2, 1) dissociation channels. Moreover, the CEP-dependent asymmetries are roughly in phase with the asymmetry of the  $\text{CO}^+$  ion detected in the same experiment [see Fig. 2(c)]. Analogous asymmetry maps for the  $\text{C}^+$  and  $\text{O}^+$  fragments for  $I_0 = 3.5 \times 10^{14}$  W/cm<sup>2</sup> are shown in Fig. 3. All of the (1,0) and (0,1) channels

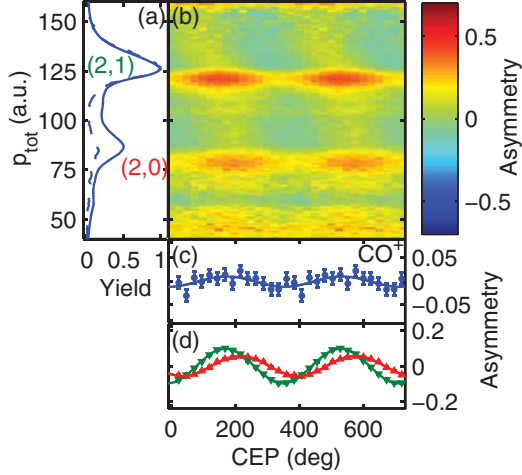


FIG. 2. (Color online) Asymmetry of the  $C^{2+}$  ion emission at  $I_0 = 1.2 \times 10^{15} \text{ W/cm}^2$ . (a) Total momentum spectra, in atomic units (a.u.), of all  $C^{2+}$  ions (solid curve) and of  $C^{2+}$  ions coincidence filtered for the (2, 1) channel (dashed curve). (b) Momentum- and CEP-resolved asymmetry of the  $C^{2+}$  ion emission, as defined by Eq. (1). (c) Asymmetry of the  $CO^+$  ion with statistical error bars calculated by assuming the error in the number of counts in the forwards (backwards) direction within each phase bin is  $\sqrt{Y_f}$  ( $\sqrt{Y_b}$ ) and then propagating this uncertainty through Eq. (1). (d) Asymmetry of the (2, 0) (red “up” triangles) and (2, 1) (green “down” triangles) channels, integrated over the ranges  $p_{\text{tot}} = 70$  to 90 a.u. and  $p_{\text{tot}} = 110$  to 130 a.u., respectively.

exhibit a phase dependent asymmetry. The low-energy  $C^+$  ions are in phase with the asymmetry in the  $CO^+$  ion, while the low-energy  $O^+$  ions are out of phase with the  $CO^+$ .

A closer look at the asymmetry maps in Figs. 2 and 3 reveals a slight momentum dependence in the phase offset of

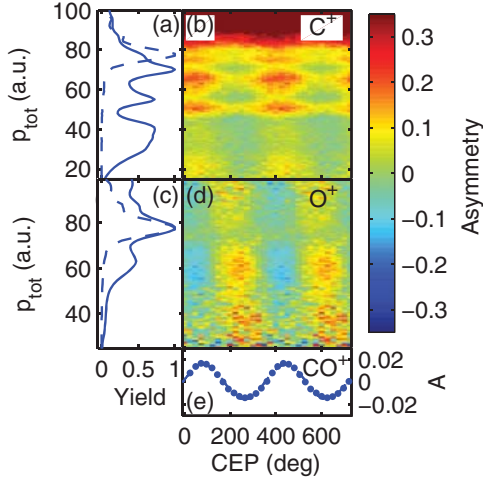


FIG. 3. (Color online) Asymmetry maps, similar to Figs. 2(a)–2(c), for the  $C^+$  [(a), (b)] and  $O^+$  [(c), (d)] ions at  $I_0 = 3.5 \times 10^{14} \text{ W/cm}^2$ . In panels (a) and (c), the total momentum spectra, in atomic units (a.u.), of all detected ions are represented as solid curves and the coincidence-filtered momentum spectra for the ions from the (1, 1) channel are represented as dashed curves. Panel (e) shows the asymmetry in the  $CO^+$  ion.

TABLE I. Asymmetry parameters for the  $(p, q)$  fragmentation channels of CO at two laser intensities. For the channels where both ions were detected, the phase shifts of both ions are reported. The last row includes phase data for the  $Ar^{2+}$  ions, which was taken as a reference immediately before or after the CO experiments in order to minimize drift in the laser conditions and the phase recovered from the phase meter. The difference in the  $Ar^{2+}$  asymmetry at low and high intensity may reflect the evolution of the predominant  $Ar^{2+}$  production path from nonsequential-to-sequential ionization or, less likely, a change in the mechanism responsible for the asymmetry in the  $CO^+$  reference. KERs (or the  $Ar^{2+}$  energy) are in eV; phase shifts relative to the  $CO^+$  ion asymmetry,  $\Delta\phi$ , are in degrees;  $A$  is the amplitude of the asymmetry parameter.  $\Delta\phi$  and  $A$  are determined by fits to the raw asymmetry data (see text for details). The uncertainty in the relative phase determination is  $\pm(1^\circ$  to  $10^\circ)$  for most channels, except for the high-intensity  $C^+$  4.0 eV (1, 0) and (1, 1) channels ( $\pm 20^\circ$ ), the high intensity  $CO^+$  species ( $\pm 32^\circ$ ), and the  $Ar^{2+}$  species ( $\pm 15^\circ$ ).

Channel	Ion	$3.5 \times 10^{14} \text{ W/cm}^2$			$1.2 \times 10^{15} \text{ W/cm}^2$		
		KER	$\Delta\phi$	$A$	KER	$\Delta\phi$	$A$
(1, 0)	$C^+$	1.0	0	0.04			
(1, 0)	$C^+$	1.8	-2	0.03	1.5	44	0.009
(1, 0)	$C^+$	3.4	-21	0.05	4.0	3	0.01
(1, 0)	$C^+$	5.2	-24	0.06			
(0, 1)	$O^+$	1.8	186	0.06			
(0, 1)	$O^+$	4.2	165	0.11			
(1, 1)	$C^+$	6.5	-33	0.03	6.2 to 9.3	-26	0.004
	$O^+$	6.5	139	0.03			
(1, 1)	$C^+$	8.1	-45	0.04			
	$O^+$	8.1	135	0.04			
(1, 1)	$C^+$	9.8	-42	0.04			
	$O^+$	9.8	144	0.05			
(2, 0)	$C^{2+}$				3.9	21	0.04
(2, 0)	$C^{2+}$				8.1	42	0.06
(2, 0)	$C^{2+}$				11.9	26	0.05
(2, 1)	$C^{2+}$				17.4	-6	0.1
	$Ar^{2+}$	0.001	132	0.35	0.001	-63	0.09

the observed asymmetry oscillation. In order to quantify the relative phase shifts between channels, we calculate a one-dimensional (1D) asymmetry curve by integrating  $Y_f$  and  $Y_b$  over a narrow momentum region. This is illustrated in Fig. 2(d), where we have integrated over momentum ranges of  $p_{\text{tot}} = 70$  to 90 a.u. and  $p_{\text{tot}} = 110$  to 130 a.u. for the (2, 0) and (2, 1) channels, respectively. This procedure is followed for all of the observed fragmentation channels, and the 1D asymmetry data is then fitted by a cosine function. The phase shifts, relative to the asymmetry in the  $CO^+$  ion (not the absolute CEP), and the amplitude of the asymmetry obtained from the fits are tabulated in Table I.

Close to the appearance intensity, the asymmetry amplitudes can be substantial. For instance, the (0, 1) channel at  $3.5 \times 10^{14} \text{ W/cm}^2$  and the (2, 1) channel at  $1.2 \times 10^{15} \text{ W/cm}^2$  have asymmetry amplitudes of  $\pm 0.1$ . However, in general, increasing the laser intensity decreases the amplitude of the asymmetry in a given channel. The amplitude of the observed asymmetry in the (1, 0) channels is somewhat smaller than

that reported previously [7], which may be due to the higher intensity used in the current work.

Throughout our analysis, we use the asymmetry in the CO<sup>+</sup> ions, collected simultaneously with the fragmentation data, as a phase reference. For the low-intensity measurements, this provides a clean reference [see Fig. 3(e)]. However, at high intensities, the CO<sup>+</sup> asymmetry is reduced, introducing a larger error in the determination of the reference phase [see Fig. 2(c)]. Regardless, we observe that low-energy C<sup>+</sup> fragments from the dissociative ionization channels are in phase with the asymmetry in the CO<sup>+</sup> ion and out of phase with the O<sup>+</sup> fragments from the (0, 1) channel. For all observed channels, the C<sup>p+</sup> fragments are emitted in the same direction, with only small phase shifts between channels.

#### IV. DISCUSSION

The relative phase shifts between fragmentation channels reflect the strong-field dynamics responsible for the different dissociation pathways. For instance, the 180° phase shift between the C<sup>+</sup> and O<sup>+</sup> fragments from the (1, 0) and (0, 1) channels suggests that both channels are formed from the same initial ionization step and laser-induced coupling between the CO<sup>+</sup> states does not significantly alter the initial asymmetry. This is in contrast to previous experiments performed at significantly lower intensity,  $8 \times 10^{13}$  W/cm<sup>2</sup> [7], where both recollisional excitation and coupling between various states influence the final asymmetry of the (1, 0) and (0, 1) channels.

Interestingly, Liu *et al.* reported a 180° phase shift between the C<sup>2+</sup> fragments from the (2, 0) and (2, 1) channels emitted into a 50° cone around the laser polarization when they exposed CO to 4 fs pulses at  $I_0 = 6 \times 10^{14}$  W/cm<sup>2</sup> [12]. They attributed this phase shift to a general, molecule-nonspecific phenomenon involving competition between recollision excitation and recollision ionization pathways. In contrast, at twice their laser intensity, we measure asymmetries of comparable amplitude but with only a very small phase shift between the (2, 0) and (2, 1) channels. Thus, the mechanism they propose is not primarily responsible for the asymmetries we observe. Rather, the similarity in the asymmetry curves for all the C<sup>p+</sup> fragments and the CO<sup>+</sup> ions might suggest that the directionality derives from the orientation dependence of the initial ionization step.

In preliminary measurements on NO, we have observed a 60° relative phase shift between the (2, 0) and (2, 1) channels, larger than the phase difference between the analogous CO channels reported here, but smaller than the 180° shift previously observed in CO [12]. The differences in the phase shifts observed for CO and NO suggest that neither the competition between recollision excitation and recollision ionization (resulting in a 180° shift) nor the anisotropy of the initial ionization step (resulting in no shift) are generally responsible for the fragmentation asymmetries of higher charge states. Instead, multielectron dissociative ionization appears to proceed through more complex, intensity- and molecule-dependent processes. Clearly, further experimental and theoretical studies are needed to better understand the source of the channel asymmetries in NO and CO and to determine if any general predictions can be made regarding analogous processes in other molecules.

#### V. SUMMARY

We have measured the CEP dependence of the directional ion emission from several fragmentation channels in CO. We find larger asymmetries when the laser intensity is nearer to the appearance intensity for a given channel. We observe relatively small phase shifts in the directional asymmetry between channels, but we do not observe the 180° phase shift between the (2, 0) and (2, 1) channels previously reported [12]. This suggests a strong laser intensity dependence of the dissociation mechanisms responsible for the (2, 0) and (2, 1) channels.

#### ACKNOWLEDGMENTS

We are grateful for support by the Max Planck Society, the Chemical Sciences, Geosciences, and Biosciences Division, Office of Basic Energy Sciences, Office of Science, US Department of Energy under DE-FG02-86ER13491 and DE-FG02-00ER15053, the National Science Foundation under CHE-0822646, the DFG via the Emmy-Noether program, the International Collaboration in Chemistry program, and the Cluster of Excellence: Munich Center for Advanced Photonics (MAP). We acknowledge support by the EU via LaserLab Europe, and N.G.J. is grateful for support by the Fulbright Commission.

- 
- [1] T. Brixner and G. Gerber, *Chem. Phys. Chem.* **4**, 418 (2003).  
 [2] M. F. Kling, Ch. Siedschlag, A. J. Verhoef, J. I. Khan, M. Schultze, Th. Uphues, Y. Ni, M. Uiberacker, M. Drescher, F. Krausz, and M. J. J. Vrakking, *Science* **312**, 246 (2006).  
 [3] M. F. Kling, Ch. Siedschlag, I. Znakovskaya, A. J. Verhoef, S. Zherebtsov, F. Krausz, M. Lezius, and M. J. J. Vrakking, *Molec. Phys.* **106**, 445 (2008).  
 [4] M. Kremer, B. Fischer, B. Feuerstein, V. L. B. de Jesus, V. Sharma, C. Hofrichter, A. Rudenko, U. Thumm, C. D. Schröter, R. Moshhammer, and J. Ullrich, *Phys. Rev. Lett.* **103**, 213003 (2009).  
 [5] B. Fischer, M. Kremer, T. Pfeifer, B. Feuerstein, V. Sharma, U. Thumm, C. D. Schröter, R. Moshhammer, and J. Ullrich, *Phys. Rev. Lett.* **105**, 223001 (2010).  
 [6] I. Znakovskaya, P. von den Hoff, G. Marcus, S. Zherebtsov, B. Bergues, X. Gu, Y. Deng, M. J. J. Vrakking, R. Kienberger, F. Krausz, R. de Vivie-Riedle, and M. F. Kling, *Phys. Rev. Lett.* **108**, 063002 (2012).  
 [7] I. Znakovskaya, P. von den Hoff, S. Zherebtsov, A. Wirth, O. Herrwerth, M. J. J. Vrakking, R. de Vivie-Riedle, and M. F. Kling, *Phys. Rev. Lett.* **103**, 103002 (2009).  
 [8] R. Weinkauff, P. Schanen, D. Yang, S. Soukara, and E. W. Schlag, *J. Phys. Chem.* **99**, 11255 (1995).

- [9] A. Hishikawa, S. Liu, A. Iwasaki, and K. Yamanouchi, *J. Chem. Phys.* **114**, 9856 (2001).
- [10] A. M. Sayler, P. Q. Wang, K. D. Carnes, B. D. Esry, and I. Ben-Itzhak, *Phys. Rev. A* **75**, 063420 (2007).
- [11] B. Gaire, J. McKenna, A. M. Sayler, N. G. Johnson, E. Parke, K. D. Carnes, B. D. Esry, and I. Ben-Itzhak, *Phys. Rev. A* **78**, 033430 (2008).
- [12] Y. Liu, X. Liu, Y. Deng, C. Wu, H. Jiang, and Q. Gong, *Phys. Rev. Lett.* **106**, 073004 (2011).
- [13] J. Ullrich, R. Moshhammer, A. Dorn, R. Dörner, L. Ph. H. Schmidt, and H. Schmidt-Böcking, *Rep. Prog. Phys.* **66**, 1463 (2003).
- [14] T. Wittmann, B. Horvath, W. Helml, M. G. Schätzel, X. Gu, A. L. Cavalieri, G. G. Paulus, and R. Kienberger, *Nat. Phys.* **5**, 357 (2009).
- [15] N. G. Johnson, O. Herrwerth, A. Wirth, S. De, I. Ben-Itzhak, M. Lezius, B. Bergues, M. F. Kling, A. Senftleben, C. D. Schröter, R. Moshhammer, J. Ullrich, K. J. Betsch, R. R. Jones, A. M. Sayler, T. Rathje, K. Rühle, W. Müller, and G. G. Paulus, *Phys. Rev. A* **83**, 013412 (2011).
- [16] M. Schultze, A. Wirth, I. Grguras, M. Uiberacker, T. Uphues, A. J. Verhoef, J. Gagnon, M. Hofstetter, U. Kleineberg, E. Goulielakis, and F. Krausz, *J. Electron. Spectrosc. Relat. Phenom.* **184**, 68 (2011).
- [17] T. Rathje, N. G. Johnson, M. Möller, F. Süßmann, D. Adolph, M. Kübel, R. Kienberger, M. F. Kling, G. G. Paulus, and A. M. Sayler, *J. Phys. B* **45**, 074003 (2012).
- [18] M. Kübel, K. J. Betsch, N. G. Johnson, U. Kleineberg, R. Moshhammer, J. Ullrich, G. G. Paulus, M. F. Kling, and B. Bergues, *New J. Phys.* **14**, 093027 (2012).
- [19] A. Rudenko, K. Zrost, B. Feuerstein, V. L. B. de Jesus, C. D. Schröter, R. Moshhammer, and J. Ullrich, *Phys. Rev. Lett.* **93**, 253001 (2004).
- [20] O. Herrwerth, A. Rudenko, M. Kremer, V. L. B. de Jesus, B. Fischer, G. Gademann, K. Simeonidis, A. Achtelik, Th. Ergler, B. Feuerstein, C. D. Schröter, R. Moshhammer, and J. Ullrich, *New J. Phys.* **10**, 025007 (2008).
- [21] B. Bergues, M. Kübel, N. G. Johnson, B. Fischer, N. Camus, K. J. Betsch, O. Herrwerth, A. Senftleben, A. M. Sayler, T. Rathje, T. Pfeifer, I. Ben-Itzhak, R. R. Jones, G. G. Paulus, F. Krausz, R. Moshhammer, J. Ullrich, and M. F. Kling, *Nat. Commun.* **3**, 813 (2012).
- [22] S. De, M. Magrakvelidze, I. A. Bocharova, D. Ray, W. Cao, I. Znakovskaya, H. Li, Z. Wang, G. Laurent, U. Thumm, M. F. Kling, I. V. Litvinyuk, I. Ben-Itzhak, and C. L. Cocke, *Phys. Rev. A* **84**, 043410 (2011).
- [23] M. Lundqvist, P. Baltzer, D. Edvardsson, L. Karlsson, and B. Wannberg, *Phys. Rev. Lett.* **75**, 1058 (1995).
- [24] S. Hsieh and J. H. D. Eland, *J. Phys. B* **29**, 5795 (1996).
- [25] G. Dawber, A. G. McConkey, L. Avaldi, M. A. MacDonald, G. C. King, and R. I. Hall, *J. Phys. B* **27**, 2191 (1994).
- [26] J. McKenna, A. M. Sayler, F. Anis, N. G. Johnson, B. Gaire, U. Lev, M. A. Zohrabi, K. D. Carnes, B. D. Esry, and I. Ben-Itzhak, *Phys. Rev. A* **81**, 061401(R) (2010).
- [27] D. L. Hatten, J. Zhu, J. Goldhar, and W. T. Hill III, *Laser Phys.* **7**, 858 (1997).
- [28] P. von den Hoff, I. Znakovskaya, M. F. Kling, and R. de Vivie-Riedle, *Chem. Phys.* **366**, 139 (2009).